RSC Advances

PAPER

View Article Online
View Journal | View Issue

Cite this: *RSC Adv.*, 2019, **9**, 10645

EDTA-bonded multi-connected carbon-dots and their Eu^{3+} complex: preparation and optical properties

Tianhao Ji, *[a] Peidong Fan,[a] Xueli Li,[a] Zhipeng Mei,[b] Yongyun Mao[b] and Yanqing Tian[b]

EDTA-bonded multi-connected carbon-dots (EDTA–C-dots) were prepared from carbon dot precursors and complexed with Eu^{3+} to give Eu^{3+}-coordinated EDTA-bonded multi-connected carbon dots (Eu–EDTA–C-dots). Whereas EDTA–C-dots were readily soluble in DMSO, Eu–EDTA–C-dots could not be easily dissolved in DMSO, water, or other common organic solvents. The newly prepared materials were thoroughly characterized. The X-ray diffraction results showed that no crystalline phase of Eu oxides (europium oxide or europium hydroxide) could be observed in Eu–EDTA–C-dots. The infrared and UV-Vis spectra showed that coordination with Eu^{3+} ions did not damage the structure of the EDTA–C-dots. It was found that EDTA could be easily grafted on the surface of carbon dots and EDTA had minimal influence on the photoluminescence of the carbon dot matrix. In contrast, the existence of Eu^{3+} ions strongly quenched the photoluminescence of Eu–EDTA–C-dots. The measured and fitted decay lifetime indicated that Eu–EDTA–C-dots possessed two photoluminescence decay processes, *i.e.*, radiative recombination and non-radiative recombination.

Received 28th February 2019
Accepted 19th March 2019

DOI: 10.1039/c9ra01521c

rsc.li/rsc-advances

1 Introduction

Carbon dots (C-dots) include all kinds of fluorescent carbon nanoparticles having a particle diameter of <10 nm. The term was first proposed in 2006 by Sun *et al.*[1] and received escalating attention in the subsequent decade.[2–6] Carbon dots have been successfully exploited as optical materials in diverse applications, *e.g.*, in studying cytotoxicity and biocompatibility,[7–9] bioimaging,[6,10,11] drug delivery,[12–15] photocatalysis,[16] photothermal therapy,[17–19] photocurrent and photovoltaics,[20,21] metal ion detection,[5,22–31] H_2O_2 detection,[32] *etc.*

The detection of metal ions with C-dots, as a kind of promising fluorometric nanosensor, has been investigated extensively.[5,22,23] For instance, the detection of Fe^{3+}, Hg^{2+}, and Cu^{2+} has been achieved based on the fluorescent quenching of the C-dots nanosensor.[22–26] Since coexisting Fe^{3+} and Hg^{2+} in aqueous solution could interfere with each other, Liu *et al.* studied the detection of metal ions in the mixture solution of Hg^{2+} and Fe^{3+}, and demonstrated that C-dots could also be effectively utilized in the presence of SCN^- and $P_3O_{10}^{5-}$ anions.[27] Also, to improve the sensitivity of Hg^{2+} detection in water, Chen *et al.* prepared C-dots/Au-clusters nanocomposite and studied corresponding ratiometric fluorescence in detail.[28] In addition, non-transition metal ions (*e.g.* K^+,[26] Al^{3+},[27] Bi^{3+}, and Sn^{2+}) could also be detected using C-dots.[31]

The detection of rare earth elements with C-dots has been relatively less reported. Singhal *et al.* used Eu-coordinated C-dots to detect F^- ions,[33] and indicated that the Eu^{3+} ions interacted relatively loosely with the carboxylic acid moiety on the C-dots. Kailasa *et al.* recently reported that Eu^{3+} hybrid C-dots could be used as a fluorescent nanosensor to detect Hg^{2+} ions,[34] but in their sensor the Eu^{3+} ions did not directly coordinate with the C-dots. Besides the application of C-dots with Eu^{3+} as detector, it should be also considered to extend to other field, and first of all, Eu^{3+} ions need be firmly bonded with C-dots.

Highly fluorescent C-dots can be synthesized from different organic precursors including citric acid, EDTA salts,[35] or graphene,[36,37] but it remains challenging to bond C-dots firmly with rare-earth ions. To our knowledge, nobody has obtained EDTA-bonded C-dots, which can be bonded easily with Eu^{3+} ions. In this work, based on the synthesis of EDTA-bonded multi-connected C-dots (referred to as EDTA–C-dots), Eu-coordinated EDTA–C-dots were successfully prepared through a simple procedure and were then characterized systemically.

2 Materials and methods

2.1 Materials

All reagents were of analytical reagent grade and used without further purification. 1-Ethyl-3-(3-dimethylaminopropyl)

[a]*Science College, Beijing Technology and Business University, Beijing 100048, China. E-mail: jitianhao@th.btbu.edu.cn*

[b]*Department of Materials Science and Engineering, Southern University of Science and Technology, Shenzhen 518055, China*

carbodiimide hydrochloride (EDC) and *N*-hydroxysulfosuccinimide sodium salt (S-NHS) were purchased from Aladdin. $Eu(NO_3)_3 \cdot 6H_2O$ (99.9%), ethylene diamine tetraacetic acid (EDTA), citric acid, ethylenediamine, and dimethylsulfoxide (DMSO) were purchased from Sinopharm.

2.2 Methods

Preparation of EDTA-free x-C-dots. The precursor carbon dots (C-dots) were prepared from citric acid and ethylenediamine in autoclave as described in the literature report,[38] and subsequently as comparison, multi-connected C-dots (referred to as x-C-dots) were synthesized at room temperature as follows. 0.35 g of EDC (1.82 mmol) and 0.20 g of S-NHS (0.91 mmol) was sequentially added into a solution with the C-dots powder (0.20 g) and DMSO (20 mL) under magnetic stirring. The resulting homogeneous solution was stirred at ambient temperature for one day before the addition of 150 mL ethanol, which rapidly gave a suspension. The suspension was centrifuged and washed with ethanol for four times to give the EDTA-free x-C-dots.

Synthesis of EDTA–C-dots and Eu–EDTA–C-dots. To the solution of C-dots (0.20 g) in DMSO (60 mL) was successively added EDTA (0.35 g), EDC (0.12 g), and S-NHS (0.06 g). The mixture was stirred at ambient temperature for one day before the addition of ethanol (150 mL), and the precipitated EDTA–C-dots were washed with ethanol for four time, and then treated under vacuum at about 40 °C.

To the solution of the obtained EDTA–C-dots (0.07 g) in DMSO (50 mL) was added $Eu(NO_3)_3 \cdot 6H_2O$ (0.012 g) under stirring at room temperature. The mixture was then stirred at ambient temperature for one day before the addition of ethanol (100 mL), and the precipitated Eu–EDTA–C-dots suspension was collected by centrifugation and washed with ethanol for four times. After treated under vacuum, the product was stored at room temperature. The Eu^{3+} content in the Eu–EDTA–C-dots was analyzed by ICP-MS to be about 11.9 wt%.

Fig. 1 gives the schematic illustration of the preparation of EDTA–C-dots and Eu–EDTA–C-dots, along with one HRTEM image of the precursor C-dots (~2.5 nm in particle diameter).

Measurements and characterization. The UV-Vis absorption spectra were measured on an Agilent Cary-60 UV-Vis spectrophotometer. The photoluminescence (PL) spectra of the samples in quartz cells were recorded on a Cary Eclipse fluorescence spectrophotometer using a Xe lamp as the excitation source in the same condition of measurements. The Fourier transform infrared (FTIR) spectra were measured on a Thermo Scientific IR spectrophotometer. The X-ray powder diffraction (XRD) analysis was performed on a Bruker AXS-D2 diffractometer with Cu Kα radiation (λ = 1.5406 Å). The transmission electron microscope (TEM) images were recorded on a Tecnai F30 instrument. The Eu^{3+} content in Eu–EDTA–C-dots was measured on an Agilent-7900cx inductively coupled plasma mass spectrometer (ICP-MS). The decay lifetime of the samples was measured at room temperature using a DeltaFlex ultrafast lifetime spectrofluorometer.

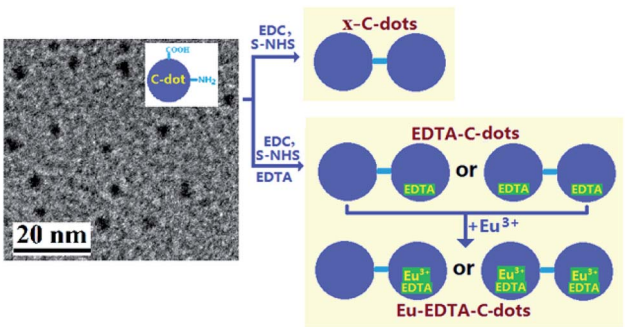

Fig. 1 Schematic illustration of the preparation process of EDTA–C-dots and Eu–EDTA–C-dots. In the inset, there includes one HRTEM image of precursor C-dots with about 2.5 nm of particle diameter.

3 Results and discussion

3.1 Characterization of C-dots and x-C-dots

In the FTIR spectra of the precursor C-dots and EDTA-free x-C-dots (Fig. 2A), the amide I and amide II bands appeared at around 1690 and 1550 cm^{-1}, which in combination with the vibration absorptions of C=O and N–H bands[39] confirmed the presence of the –NHCO– linker in the two samples.[40] The absorption peak at around 1020 cm^{-1} could be assigned to the C–O stretching vibration.[41] In addition, C-dots and x-C-dots had similar UV-Vis spectra (Fig. 2B), indicating that the x-C-dots were made of the C-dots. However, their PL spectra differed strikingly because the electron–hole state of various groups on the material surface (*e.g.* –COOH, $-NH_2$, and –NHCO–) had changed after the reaction.[42] The x-C-dots showed the strongest PL intensity under excitation at 340 nm, and aside from the primary fluorescent peak at 480 nm, there was also a broad fluorescent peak at about 430 nm. In contrast, the precursor C-dots had the strongest PL intensity under excitation at 365 nm, and only gave one fluorescent peak at 450 nm without broadening. It could be inferred that the surface groups with PL behaviors underwent certain changes after they were subjected to the reaction conditions (*i.e.*, exposure to EDC and NHS).

3.2 Characterization of EDTA–C-dots and Eu–EDTA–C-dots

Similarly, EDTA-bonded multi-connected C-dots (EDTA–C-dots) were prepared and further coordinated with Eu^{3+} to give Eu–EDTA–C-dots. Before the complexation produced, the EDTA–C-dots could be dissolved in DMSO, and whereas it was found that Eu–EDTA–C-dots hardly dissolved in water or other common organic solvents (*e.g.*, DMSO, DMF, ethanol, acetone). X-ray diffraction analysis confirmed that Eu oxides did not exist in the Eu–EDTA–C-dots (Fig. 3A).

The complexation between EDTA–C-dots and Eu^{3+} could also be confirmed by FTIR measurements (Fig. 3B). Since the IR spectrum of the EDTA–C-dots was similar to that of x-C-dots, it could be reasoned that the reaction of EDTA with C-dots barely affected the structure of the C-dots. The amide I and amide II bands at around 1692 cm^{-1} and 1545 cm^{-1} in the EDTA–C-dots also proved the existence of the –OCNH– linker.[39] In comparison, the absorption pattern of the Eu–EDTA–C-dots in 1500–

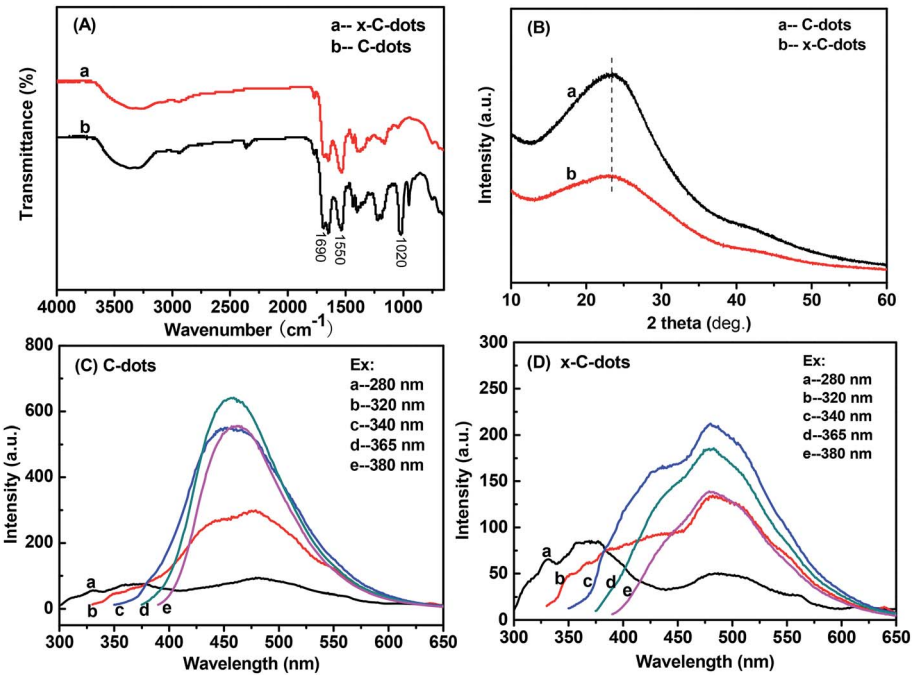

Fig. 2 Characterizations of precursor C-dots and EDTA-free x-C-dots: (A) FTIR spectra; (B) XRD patterns; (C) PL of the C-dots; (D) PL of the x-C-dots.

1700 cm^{-1} differed prominently, and the notable peak broadening in this area could be attributed to the coordination of the Eu^{3+} ions.[43] It could be inferred that the complexation between Eu^{3+} ions and EDTA–C-dots changed both the state of valence electrons and the bond length in the amide linker.

The morphologies of the EDTA–C-dots and Eu–EDTA–C-dots could be clearly observed from their TEM images (Fig. 3C and D). Under the preparation condition of the EDTA–C-dots, the precursor C-dots appear obvious aggregation due to the reaction between different C-dots with each other, supported by the TEM

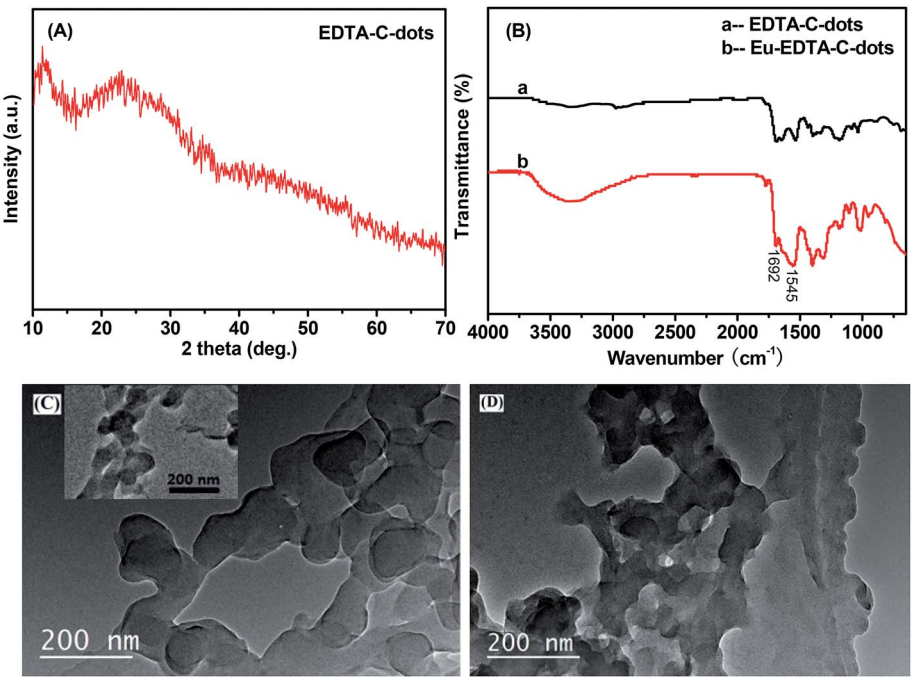

Fig. 3 (A) XRD pattern of Eu–EDTA–C-dots; (B) FTIR spectra of EDTA–C-dots and Eu–EDTA–C-dots; (C) TEM image of EDTA–C-dots; (D) TEM image of Eu–EDTA–C-dots. Inset in (C) is the TEM image of precursor x-C-dots.

image of x-C-dots and below PL results. Similar to the TEM image of the EDTA–C-dots, the TEM image of the x-C-dots in the inset also shows serious aggregation, inferring the morphology of the EDTA–C-dots may result from the reaction between C-dots. In fact, it should be easily understood that because the co-existence of –COOH and $-NH_2$ groups on the surface of each carbon-dot, C-dots can also react with each other under the synthesis of EDTA–C-dots. The coordination of Eu^{3+} ions still remain similar aggregation state, and the solubility proves that such Eu-complex possesses much serious aggregation.

3.3 Optical properties of EDTA–C-dots and Eu–EDTA–C-dots

The UV-Vis absorptions of the EDTA–C-dots and Eu–EDTA–C-dots (Fig. 4) were similar except for the slight redshift of the absorption peak of Eu–EDTA–C-dots, indicating that the complexation of Eu^{3+} hardly affected the structure of the EDTA–C-dot ligands. The PL spectra of the EDTA–C-dots and Eu–EDTA–C-dots under excitation at 340 nm (Fig. 4 inset) differed obviously in 400–600 nm. After the coordination of Eu^{3+} with Eu–EDTA–C-dots, the PL peak at 480 nm experienced serious fluorescence quenching, due to the energy transfer of the non-radiative recombination between Eu^{3+} ions and C-dots.

The PL behaviors of EDTA–C-dots and Eu–EDTA–C-dots upon different excitations were further inspected (Fig. 5). The PL spectrum of the EDTA–C-dots was similar to that of x-C-dots (Fig. 5A), further demonstrating that grafting EDTA on the surface of x-C-dots did not destroy the surface fluorescent groups. The strongest fluorescent peak (at ~480 nm) of EDTA–C-dots was observed when excitation was applied at 340 nm. In contrast, the addition of Eu^{3+} obviously quenched the strong PL emission at ~480 nm, probably due to energy transfer quenching *via* non-radiative recombination between Eu^{3+} ions and C-dots (elaborated below further in the lifetime measurements). Similar quenching was previously observed for Au@C-dots or C-dots/ZnO[44,45] in the presence of Fe^{3+}, Hg^{2+}, or Pb^{2+} ions.[46–48]

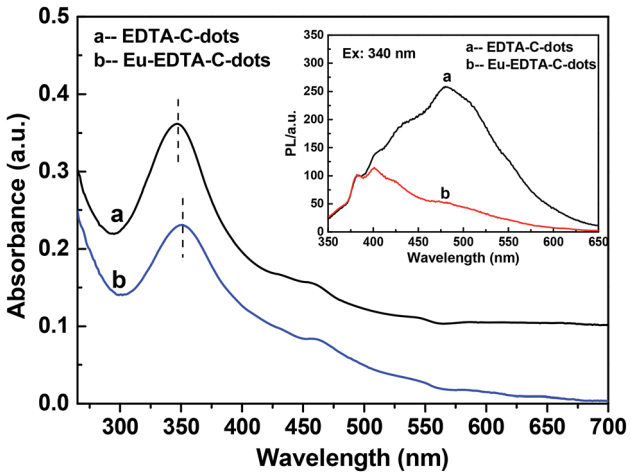

Fig. 4 UV-Vis absorption spectra of EDTA–C-dots and Eu–EDTA–C-dots. Inset is the PL spectra of the EDTA–C-dots and Eu–EDTA–C-dots under 340 nm of excitation wavelength.

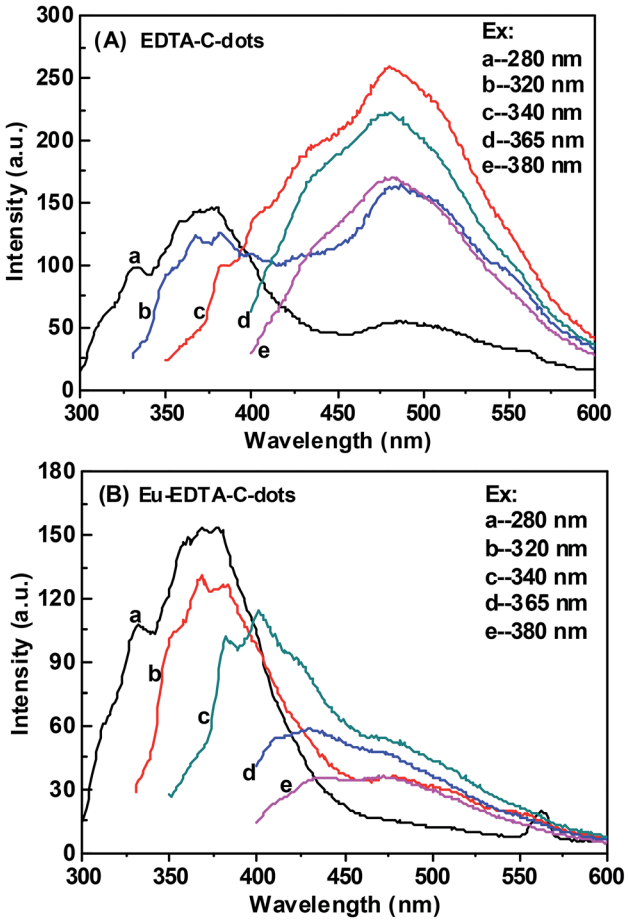

Fig. 5 Photoluminescence spectra of EDTA–C-dots and Eu–EDTA–C-dots under different excitation wavelength.

3.4 Luminescent decay spectra of EDTA–C-dots and Eu–EDTA–C-dots

The luminescent decay spectra of EDTA–C-dots and Eu–EDTA–C-dots subjected to excitation at 340 nm revealed the transfer

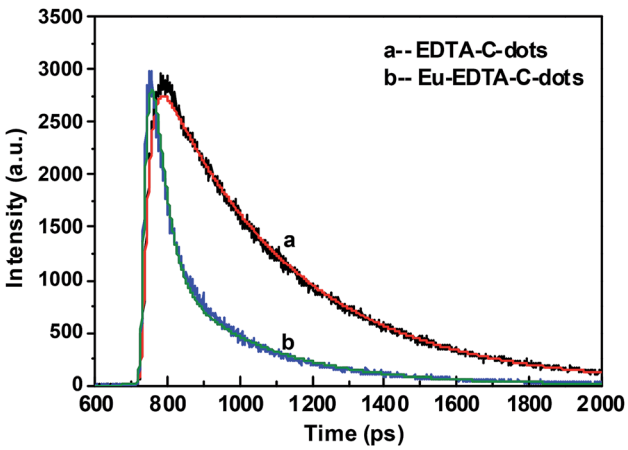

Fig. 6 Luminescence decay spectra of EDTA–C-dots (a) and Eu–EDTA–C-dots (b) with 340 nm of excitation wavelength.

properties of the photo-induced electron (Fig. 6). The PL decay (exciton lifetime) of EDTA–C-dots was measured to be 9.47 ns and could be single-exponentially fitted to be 9.83 ns. In contrast, Eu–EDTA–C-dots had a measured PL decay of 2.47 and 9.86 ns that could be double-exponentially fitted to be 0.85 and 7.13 ns, respectively. Since the C-dot precursor was reported to have a short PL decay of about 3.6 ns,[49] the longer exciton lifetime of EDTA–C-dots probably resulted from the radiative recombination between linked C-dots. In contrast, Eu–EDTA–C-dots showed two obviously distinct exciton lifetimes, probably because two kinds of processes were involved in the decay, *i.e.*, radiative recombination between linked C-dots and non-radiative recombination between C-dot and Eu^{3+}.

4 Conclusions

In this work, we prepared and characterized EDTA-bonded multi-connected carbon dots (EDTA–C-dots) and Eu^{3+}-coordinated EDTA-bonded multi-connected carbon dots (Eu–EDTA–C-dots). We found that EDTA–C-dots readily dissolved in DMSO but Eu–EDTA–C-dots could not be easily dissolved in DMSO, water, or other common organic solvents. In preparing EDTA–C-dots, the –COOH and $-NH_2$ groups on the surface of the precursor C-dots not only reacted with the added EDTA but also reacted with each other. The attachment of EDTA barely affected the photoluminescence (PL) properties of the carbon dots, but the existence of Eu^{3+} ions in Eu–EDTA–C-dots notably quenched the fluorescence, which suggested the occurrence of non-radiative processes between the carbon dots and the Eu^{3+} ions. The measured and fitted PL decay of Eu–EDTA–C-dots showed two decay lifetimes, which corresponded to two kinds of electron transfer processes, *i.e.*, radiative recombination and non-radiative recombination.

Conflicts of interest

There are no conflicts to declare.

Acknowledgements

This work was funded by the funding of the Agricultural Environmental Monitoring Station of Beijing (No. 19000551347) and the National Natural Science Foundation of China (No. 21774054). Authors are grateful to Prof. H. Yang and J. Sun, working in the Engineering College of Peking University, for the measurement of PL lifetime.

References

1 Y. P. Sun, B. Zhou, Y. Lin, W. Wang, K. A. S. Fernando, P. Pathak, M. J. Meziani, B. A. Harruff, X. Wang, H. Wang, P. G. Luo, H. Yang, M. E. Kose, B. Chen, L. M. Veca and S. Y. Xie, *J. Am. Chem. Soc.*, 2006, **128**, 7756–7757.
2 X. Wang, L. Cao, F. S. Lu, M. J. Meziani, H. T. Li, G. Qi, B. Zhou, B. A. Harruff, F. Kermarrec and Y. P. Sun, *Chem. Commun.*, 2009, 3774–3776.
3 R. L. Liu, D. Q. Wu, S. H. Liu, K. Koynov, W. Knoll and Q. Li, *Angew. Chem., Int. Ed.*, 2009, **48**, 4598–4601.
4 P. Anilkumar, X. Wang, L. Cao, S. Sahu, J. H. Liu, P. Wang, K. Korch, K. N. Tackett, A. Parenzan and Y. P. Sun, *Nanoscale*, 2011, **3**, 2023–2027.
5 Q. Song, Y. S. Ma, X. Wang, T. Tang, Y. Y. Song, Y. J. Ma, G. H. Xu, F. D. Wei, Y. Cen and Q. Hu, *J. Colloid Interface Sci.*, 2018, **516**, 522–528.
6 Y. Y. Yang, X. F. Wang, G. C. Liao, X. Q. Liu, Q. L. Chen, H. M. Li, L. Lu, P. Zhao and Z. Q. Yu, *J. Colloid Interface Sci.*, 2018, **509**, 515–521.
7 E. J. Goh, K. S. Kim, Y. R. Kim, H. S. Jung, S. Beack, W. H. Kong, G. Scarcelli, S. H. Yun and S. K. Hahn, *Biomacromolecules*, 2012, **13**, 2554–2561.
8 W. Wang, L. Cheng and W. G. Liu, *Sci. China: Chem.*, 2014, **57**, 522–539.
9 N. Zhou, Z. Y. Hao, X. H. Zhao, S. Maharjan, S. J. Zhu, Y. B. Song, B. Yang and L. Lu, *Nanoscale*, 2015, **7**, 15635–15642.
10 V. B. Kumar, J. Sheinberger, Z. Porat, Y. Shav-Tal and A. Gedanken, *J. Mater. Chem. B*, 2016, **4**, 2913–2920.
11 R. Y. Li, X. Wang, Z. J. Li, H. Y. Zhu and J. K. Li, *New J. Chem.*, 2018, **42**, 4352–4360.
12 S. H. Li, D. Amat, Z. L. Peng, S. Vanni, S. Raskin, G. D. Angulo, A. M. Othman, R. M. Graham and R. M. Leblanc, *Nanoscale*, 2016, **8**, 16662–16669.
13 B. B. Wang, S. J. Wang, Y. F. Wang, Y. Lv, H. Wu, X. J. Ma and M. Q. Tan, *Biotechnol. Lett.*, 2016, **38**, 191–201.
14 R. K. Singh, K. D. Patel, C. Mahapatra, M. S. Kang and H. W. Kim, *ACS Appl. Mater. Interfaces*, 2016, **8**, 24433–24444.
15 Z. L. Peng, E. H. Miyanji, Y. Q. Zhou, J. Pardo, S. D. Hettiarachchi, S. H. Li, P. L. Blackwelder, I. Skromne and R. M. Leblanc, *Nanoscale*, 2017, **9**, 17533–17543.
16 R. Wang, K. Q. Lu, Z. R. Tang and Y. J. Xu, *J. Mater. Chem. A*, 2017, **5**, 3717–3734.
17 C. S. Hou, S. Q. Chen and M. Q. Wang, *Dalton Trans.*, 2018, **47**, 1777–1781.
18 Z. Liu, Q. Xu, Y. H. Li and W. Chen, *Mater. Chem. Front.*, 2017, **1**, 538–541.
19 M. Thakur, M. K. Kumawat and R. Srivastava, *RSC Adv.*, 2017, **7**, 5251–5261.
20 M. K. Barman, P. Mitra, R. Bera, S. Das, A. Pramanik and A. Parta, *Nanoscale*, 2017, **9**, 6791–6799.
21 J. B. Essner and G. A. Baker, *Environ. Sci.: Nano*, 2017, **4**, 1216–1263.
22 X. H. Gao, C. Du, Z. H. Zhuang and W. Chen, *J. Mater. Chem. C*, 2016, **4**, 6927–6945.
23 V. Sharma, P. Tiwari and S. M. Mobin, *J. Mater. Chem. B*, 2017, **5**, 8904–8924.
24 S. N. Qu, H. Chen, X. M. Zheng, J. S. Cao and X. Y. Liu, *Nanoscale*, 2013, **5**, 5514–5518.
25 C. Yuan, B. H. Liu, F. Liu, M. Y. Han and Z. P. Zhang, *Anal. Chem.*, 2014, **86**, 1123–1130.
26 A. Salinas-Castillo, M. Ariza-Avidad, C. Pritz, M. Camprubi-Robles, B. Fernandez, M. J. Ruedas-Rama, A. Megia-Fernández, A. Lapresta-Fernández, F. Santoyo-Gonzalez,

A. Schrott-Fischer and L. F. Capitan-Vallve, *Chem. Commun.*, 2013, **49**, 1103–1105.
27 Y. Liu, Y. N. Liu, J. P. Lee, J. H. Lee, M. Park and H. Y. Kim, *Analyst*, 2017, **142**, 1149–1156.
28 W. Liu, X. Y. Wang, Y. Q. Wang, J. H. Li, D. Z. Shen, Q. Kang and L. X. Chen, *Sens. Actuators, B*, 2018, **262**, 810–817.
29 L. Y. Zhang, S. N. Chen, Q. Zhao and H. W. Huang, *Anal. Chim. Acta*, 2015, **880**, 130–135.
30 F. Qu, S. Wang, D. Y. Liu and J. M. You, *RSC Adv.*, 2015, **5**, 82570–82575.
31 S. N. A. M. Yazid, S. F. Chin, S. C. Pang and S. M. Ng, *Microchim. Acta*, 2013, **180**, 137–143.
32 D. D. Chen, X. M. Zhuang, J. Zhai, Y. Y. Zheng, H. Lu and L. X. Chen, *Sens. Actuators, B*, 2018, **255**, 1500–1506.
33 P. Singhal, B. G. Vats, S. K. Jha and S. Neogy, *ACS Appl. Mater. Interfaces*, 2017, **9**, 20536–20544.
34 M. L. Desai, S. Jha, H. Basu, R. K. Singhal, P. K. Sharma and S. K. Kailasa, *New J. Chem.*, 2018, **42**, 6125–6133.
35 D. Y. Pan, J. C. Zhang, Z. Li, C. Wu, X. M. Yan and M. H. Wu, *Chem. Commun.*, 2010, **46**, 3681–3683.
36 L. A. Ponomarenko, F. Schedin, M. I. Katsnelson, R. Yang, E. W. Hill, K. S. Novoselov and A. K. Geim, *Science*, 2008, **320**, 356–358.
37 K. A. Ritter and J. W. Lyding, *Nat. Mater.*, 2009, **8**, 235–242.
38 S. J. Zhu, Q. N. Meng, L. Wang, J. H. Zhang, Y. B. Song, H. Jin, K. Zhang, H. C. Sun, H. Y. Wang and B. Yang, *Angew. Chem., Int. Ed.*, 2013, **52**, 3953–3957.
39 Y. P. Shi, Y. Pan, H. Zhang, Z. M. Zhang, M. J. Li, C. Q. Yi and M. S. Yang, *Biosens. Bioelectron.*, 2014, **56**, 39–45.
40 W. J. Liu, C. Li, Y. J. Ren, X. B. Sun, W. Pan, Y. H. Li, J. P. Wang and W. J. Wang, *J. Mater. Chem. B*, 2016, **4**, 5772–5788.
41 X. Cui, L. Zhu, J. Wu, Y. Hou, P. Y. Wang, Z. Wang and M. Yang, *Biosens. Bioelectron.*, 2015, **63**, 506–512.
42 L. Cao, M. J. Meziani, S. Sahu and Y. P. Sun, *Acc. Chem. Res.*, 2012, **46**, 171–180.
43 S. Y. Lu, J. Sun, Y. Wang, W. S. Yu, M. T. Sun and S. Y. Cui, *J. Rare Earths*, 2018, **36**, 669–674.
44 E. Priyadarshini and K. Rawat, *J. Mater. Chem. B*, 2017, **5**, 5425–5432.
45 M. K. Barman, P. Mitra, R. Bera, S. Das, A. Pramanik and A. Parta, *Nanoscale*, 2017, **9**, 6791–6799.
46 H. J. Zhang, Y. L. Chen, M. J. Liang, L. F. Xu, S. D. Qi, H. L. Chen and X. G. Chen, *Anal. Chem.*, 2014, **86**, 9846–9852.
47 R. H. Liu, H. T. Li, W. Q. Kong, J. Liu, Y. Liu, C. Y. Tong, X. Zhang and Z. H. Kang, *Mater. Res. Bull.*, 2013, **48**, 2529–2534.
48 S. S. Wee, Y. H. Ng and S. M. Ng, *Talanta*, 2013, **116**, 71–76.
49 P. A. Sajid, S. S. Chetty, S. Praneetha, A. V. Murugan, Y. Kumar and L. Periyasamy, *RSC Adv.*, 2016, **6**, 103482–103490.